# Microrheological Modeling of Flow-Induced Crystallization

**Salvatore Coppola and Nino Grizzuti***

*Dipartimento di Ingegneria Chimica, Università di Napoli "Federico II", Piazzale Tecchio 80, I-80125 Napoli, Italy*

**Pier Luca Maffettone**

*Dipartimento di Scienza dei Materiali e Ingegneria Chimica, Politecnico di Torino, Corso Duca degli Abruzzi 24, I-10129, Torino, Italy*

*Received February 14, 2001*

ABSTRACT: The problem of flow-induced crystallization (FIC) of polymer melts is addressed via a microrheological approach. In particular, the Doi−Edwards model with the so-called independent alignment approximation (DE−IAA) is used to calculate the flow-induced change of free energy. Subsequently, the crystallization induction time, i.e., the nucleation characteristic time, is calculated in isothermal steady shear and uniaxial elongational flows. Asymptotic, analytical expressions for the induction time are also derived in the limit of low and high Deborah number (the product of the deformation rate and the polymer relaxation time). The DE−IAA model is found to give more realistic predictions than those of simpler, dumbbell-like models already proposed in the literature. When compared to existing FIC experimental data in shear flow, good quantitative agreement is found with the polymer relaxation time as the only adjustable parameter of the model.

## 1. Introduction

When a thermoplastic semicrystalline polymer is subjected to flow, as invariably happens during processing, the crystallization rate is enhanced. This phenomenon, usually referred to as flow-induced crystallization (FIC), crucially affects both processing and material final properties.[1−3]

Polymer crystallization follows the typical two-step path of nuclei formation and subsequent growth. The flow-enhanced crystallization rate is generally attributed to a significant acceleration of the first step, i.e., the nucleation rate.[4,5]

In the classical thermodynamic approach,[6,7] the rate of nucleation in quiescent conditions depends on the free energy difference between the crystalline and the amorphous phase. The effect of flow on the nucleation kinetics can be understood by considering that the increase of the degree of order due to flow results in an effective change of the melt free energy. On the basis of this concept, several modeling approaches have been proposed in the literature. Empirical models[8−10] directly relate the free energy change to some measure of the flow intensity. Although successful in describing FIC phenomena, such models are often limited to the description of particular flow conditions and generally rely on the estimate of adjustable parameters. In recent years, increasing attention has been paid to microrheological modeling of the FIC. Models describing the polymeric liquid on a molecular basis[11] have progressively gained consensus over those based on the classical rubber elasticity theory.[12,13] Within this framework, dumbbell-like models have been initially used to calculate the flow-induced change in free energy and the subsequent crystallization rate enhancement.[14] Recently, a two-phase approach has been proposed, where the amorphous phase is described by an ensemble of dumbbells and crystallites are treated as rigid rods.[15] It has been shown that the model is capable of predicting the experimental results of an injection-molding process with a limited number of adjustable parameters.[16]

The present work is an attempt to describe isothermal FIC by microrheological modeling. The starting point is the Doi−Edwards (DE) model, which is known to successfully describe most of the rheological features of high molecular weight polymer melts.[17] In particular, the expression for the free energy under flow conditions is calculated under the so-called independent alignment approximation (IAA),[18] and is used to estimate the crystallization induction time, i.e., the nucleation characteristic time. The predictions of the model are compared with experimental data available in the literature.

## 2. Model

According to the theory of Lauritzen and Hoffman,[7] the isothermal nucleation rate for a polymer below its melting temperature can be expressed as:[19]

$$\dot{N} = CkT\Delta G \exp\left(-\frac{E_a}{kT}\right)\exp\left[-\frac{K_n}{T(\Delta G)^n}\right] \qquad (1)$$

In eq 1, $C$ includes energetic and geometrical constants, $k$ is the Boltzmann constant, $T$ the temperature, $\Delta G = G_L - G_S$ the volumetric free energy difference between liquid and crystalline phase, and $E_a$ the activation energy of the supercooled liquid nucleus interface. $K_n$ is a constant containing energetic and geometrical factors of the crystalline nucleus. The exponent $n$, appearing also as a subscript for $K$, accounts for the temperature region where the homogeneous nucleation takes place, and can generally assume the values 1 and 2.[7]

It must be stressed that eq 1 is derived under quiescent conditions. In this case, ΔG can be expressed to a good approximation as[7]

$$\Delta G = \Delta G_q = \Delta H_0\left(1 - \frac{T}{T_m}\right) \qquad (2)$$

10.1021/ma010275e CCC: $20.00 
Published on Web 06/09/2001

where $\Delta H_0$ is the latent heat of crystallization and $T_m$ the thermodynamic melting temperature. In the present work, following a commonly adopted approach, eq 1 is also used to estimate the nucleation rate under flow. In this case an additive term, $\Delta G_f$, accounts for the effect of the macroscopic flow on the free energy of the liquid phase, and $\Delta G$ assumes the form:

$$\Delta G = \Delta G_q + \Delta G_f \tag{3}$$

A constitutive equation for $\Delta G_f$, describing the effect of flow, is now required to evaluate this contribution. Once this is done, the modified free energy change obtained from eq 3 can be used in eq 1 to predict the FIC effect.

Here we propose the use of the Doi−Edwards (DE) model to calculate $\Delta G_f$. As already mentioned, the DE model is widely accepted as a realistic description of the polymer melt behavior under flow. Furthermore, it seems to possess the necessary physical ingredients to describe the FIC process. In fact, the presence of a flow field has two different effects on the polymer chains, as they can be oriented and stretched at the same time. It is well-known that in relatively slow flows (when the flow intensity is smaller than the reciprocal Rouse relaxation time) the orienting effect is dominant, stretching becoming significant at higher rates.[17,20] At the same time, experimental results[4,5,21−26] show that even small deformation rates considerably enhance the crystallization rate. This fact suggests that chain orientation could be sufficient to justify such effects, and thus supports the choice of the DE model to estimate the flow-induced free energy change. It will be shown that such a description of the crystallizing melt represents an improvement with respect to the dumbbell-like molecular models proposed so far.

In this work, the original formulation of the DE model for linear, monodisperse polymers is used. In fact, recent improvements of the model[27,28] play a major role in the nonlinear, high deformation rate limit, which is not relevant here. Furthermore, the independent alignment approximation (IAA) is adopted.[17] Such an approximation, which strongly simplifies the mathematical analysis, is known to generate only minor deviations from the rigorous model in steady flows.[17,29]

The flow-induced free energy change for the DE−IAA model was calculated, using the above assumptions, by Marrucci and Grizzuti[18] (all mathematical details can be found in the original paper). They obtained the following expression for $\Delta G_f$:

$$\Delta G_f = 3ckT \int_{-\infty}^{t} \mu(t,t')A[\mathbf{E}(t,t')]\, dt' \tag{4}$$

In eq 4, $c$ is the volumetric concentration of primitive chain segments, $\mu$ is the DE memory function:

$$\mu(t,t') = \frac{8}{\pi^2} \sum_{p\ \mathrm{odd}} \frac{1}{p^2} \exp\left[-\frac{p^2(t-t')}{T_d}\right] \tag{5}$$

where $T_d$ is the disengagement time, and $A[\mathbf{E}(t,t')]$ is given by

$$A[\mathbf{E}(t,t')] = \langle \ln[|\mathbf{E}(t,t')\cdot\mathbf{u}|]\rangle_0 \tag{6}$$

In eq 6 $\mathbf{E}(t,t')$ is the deformation history tensor between times $t'$ and $t$, $\mathbf{u}$ is the unit pseudo-vector associated with a primitive chain segment, and the symbol $\langle\cdot\rangle_0$ indicates the average over the orientational equilibrium distribution function.[18]

The chain segment concentration is equivalent to an entanglement density and can be expressed as

$$c = \frac{\rho N}{M_e} \tag{7}$$

where $\rho$ is the melt density, $N$ the Avogadro number, and $M_e$ the molecular weight between entanglements.

For steady-state uniaxial elongation and shear flow, eq 4 can be expressed as

$$\Delta G_f = 3ckT \int_0^{+\infty} \mu(z)A(\mathrm{De}\ z)\, dz \tag{8}$$

where De is the Deborah number, i.e., the deformation rate multiplied by the polymer relaxation time. Marrucci and Grizzuti[18] determined the function $A$ as

$$A(x) = \frac{1}{2}\int_0^1 \ln\left(\frac{1 + x^2\xi^2 + \sqrt{\xi^4(x^4+4x^2) - 2x^2\xi^2 + 1}}{2}\right) d\xi \tag{9}$$

for shear flow, and as

$$A(x) = x + \frac{\tan^{-1}(\sqrt{e^{3x}-1})}{\sqrt{e^{3x}-1}} - 1 \tag{10}$$

for uniaxial elongation. It should be stressed, as is apparent in eq 8, that at fixed temperature $\Delta G_f$ only depends on the entanglement density and the Deborah number.

It is instructive to investigate in details the limiting behaviors of $\Delta G_f$. Expanding eq 8 at small De yields for shear and extensional flow:

$$\frac{\Delta G_f}{3ckT} = \frac{\pi^4}{600}\mathrm{De}^2 \tag{11}$$

$$\frac{\Delta G_f}{3ckT} = \frac{\pi^4}{200}\mathrm{De}^2 \tag{12}$$

respectively. Analogously, in the high De limit:

$$\frac{\Delta G_f}{3ckT} = \ln(\mathrm{De}) - 1 - \gamma - \sum_{p\ \mathrm{odd}} \frac{\ln(p^2)}{p^2} \cong \ln \mathrm{De} - 2.41 \tag{13}$$

$$\frac{\Delta G_f}{3ckT} = \frac{\pi^2}{12}\mathrm{De} - 1 \tag{14}$$

In eq 13, $\gamma$ is the Euler gamma constant, and the series converges to about 0.83.

Despite the already mentioned limitations of the original DE−IAA model at high deformation rates, eqs 13 and 14 represent in any case an explicit estimate of the free energy change in fast flows.

The use of the DE−IAA model in predicting the FIC enhancement is straightforward. Once the flow kinematics are assigned (through the tensor $\mathbf{E}(t,t')$), $\Delta G_f$ can be directly obtained from eq 4 if the molecular weight between entanglements, $M_e$, the polymer density, $\rho$, and the disengagement time, $T_d$, are known at a specific temperature. In the next section, predictions for FIC based on the DE model will be presented.

For the sake of comparison, predictions for simpler models based on a dumbell-like description of the polymer melt will be also reported. As mentioned in the Introduction, similar models have been already used to describe the effect of flow on the crystallization kinetics.[14] Elastic dumbbell models have been initially developed to describe the rheological behavior of dilute solutions.[30] They can be extended to polymer melts by assuming that dumbbells represent macromolecule strands connecting entanglements; in this case, it can be shown their equivalence to transient network models with constant creation and destruction rate.[31] As reported by Sarti and Marrucci,[32] the flow-induced free energy change for a system of dumbbells is given by

$$\Delta G_f = ckT\left\langle \ln\frac{\psi}{\psi_0}\right\rangle \tag{15}$$

where $\psi$ is the end-to-end dumbbell distribution function, $\psi_0$ the corresponding equilibrium distribution, $c$ the number of dumbbells per unit volume, and brackets now indicate averaging over the current distribution function. It should be remarked that, for a melt represented by a network of dumbbells, $c$ corresponds to the chain segment concentration in the DE−IAA model (eq 7). The distribution function appearing in eq 15 obeys the following continuity equation:[30]

$$\frac{\partial\psi}{\partial t} = -\frac{\partial}{\partial \mathbf{R}}\cdot\left(\mathbf{K}\cdot\mathbf{R}\psi - \frac{2kT}{\zeta}\frac{\partial\psi}{\partial\mathbf{R}} - \frac{2}{\zeta}\mathbf{F}_e\psi\right) \tag{16}$$

In eq 16, $\mathbf{R}$ is the dumbbell end-to-end vector, $\mathbf{K}$ the velocity gradient, $\zeta$ the bead friction coefficient, and $\mathbf{F}_e$ the connector elastic force. $\partial/\partial\mathbf{R}$ represents the gradient operator in the $\mathbf{R}$ space. In this work, two forms for $\mathbf{F}_e$ are considered, namely, the linear elastic (LE) dumbbell, and the pre-averaged finite extendable nonlinear elastic (FENE-P) dumbbell.[33] For the LE dumbbell, $\mathbf{F}_e$ reads

$$\mathbf{F}_e = H\mathbf{R} \tag{17}$$

where $H$ is the spring elastic constant. In the FENE-P dumbbell, the connector force is defined as

$$\mathbf{F}_e = \frac{H\mathbf{R}}{1 - \left\langle\left(\frac{R}{R_0}\right)^2\right\rangle} \tag{18}$$

where $R_0$ is the dumbbell maximum length. In the case of dumbbell models, the procedure to obtain flow-enhanced crystallization predictions requires the following steps. Once the flow kinematics are assigned (through the tensor $\mathbf{K}$), the distribution function $\psi$ is calculated through eq 14, and $\Delta G_f$ is then obtained from eq 15. As for the DE−IAA model, the polymer density and the molecular weight between entanglements, are required, as well as the dumbbell relaxation time, $\tau$, defined as

$$\tau = \frac{\zeta}{4H} \tag{19}$$

For the FENE-P dumbbell, the additional nonlinear spring parameter $b = HR_0^2/kT$ is also required.[30]

## 3. Model Predictions

Figure 1 shows the dimensionless free energy change, $\Delta G_f/3ckT$, as a function of the Deborah number (De = $\dot\gamma T_d$) for a steady shear flow, as predicted by the DE−IAA model. The predictions for the dumbbell models are also shown. In the latter case, De is intended as $\dot\gamma\tau$. For the FENE-P dumbbell, a fixed value of the nonlinear constant $b = 100$ has been used. The DE−IAA model predicts the lowest increase of the free energy over a wide range of De. This is not surprising since the free-energy change for this model is purely orientational, i.e., no chain stretching is allowed. On the other hand, the transient network model with Hookean strands gives the largest free energy increase, due to the chain affine deformation. The FENE-P dumbbell predictions fall between the DE−IAA and LE dumbbell curves.

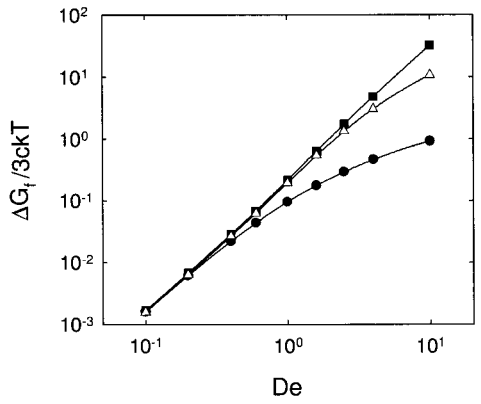


**Figure 1.** Dimensionless free energy change as a function of De for steady shear flow: (-●-) DE−IAA; (-■-) LE dumbbell; (-△-) FENE-P dumbbell with $b = 100$.

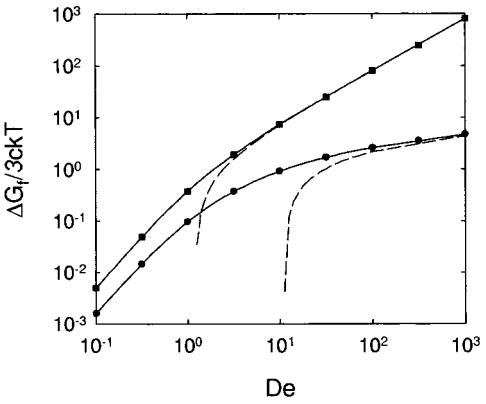


**Figure 2.** Dimensionless free energy change as a function of De for the DE−IAA model: (-●-) shear flow; (-■-) uniaxial elongation. The dashed lines are the limiting predictions for high De, eqs 13 and 14.

The same qualitative differences between DE−IAA and dumbbell models are confirmed when steady uniaxial flow is considered, and for this reason the comparison is not explicitly reported. Needless to say, in the case of the LE dumbbell the well-known divergence in the free energy is predicted for De = $\dot\epsilon\tau = {}^1/_2$, where $\dot\epsilon$ is the stretching rate, whereas no divergence is predicted by the DE−IAA model.

The different behavior in shear and elongation of the DE−IAA model is shown in Figure 2. Elongational flow is much more effective than shear in orienting the polymer chains, and obviously produces a larger $\Delta G_f$. It should be also noted from Figure 2 that the difference between elongation and shear becomes more relevant as De increases, as confirmed by comparison of eqs 13 and 14. The asymptotic trends are also reported in Figure 2 as dashed lines. It can be seen that for

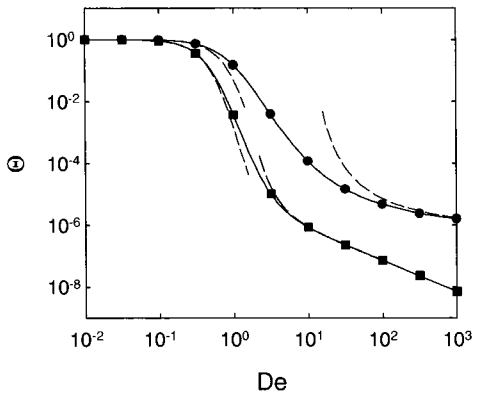


**Figure 3.** Dimensionless induction time as a function of De for the DE−IAA model: (-●-) shear flow; (-■-) uniaxial elongation. The dashed lines are the limiting predictions, eqs 21−22 and 24−25.

elongational flow the high rate approximation, eq 14, is valid for De ≥10, whereas for shear flow eq 13 holds for De ≥1000. The low De limits, eqs 11 and 12, are not reported in Figure 2. They practically coincide with the exact calculations up to De ≅ 0.5.

In most polymer FIC experiments, a characteristic time for the onset of crystallization is measured. Typically, in isothermal experiments at imposed shear rate, the time corresponding to a sudden upturn of the shear viscosity is considered.[21,25] Such a quantity, usually referred to as an "induction time", is roughly proportional to the inverse of the nucleation rate. For this reason, to estimate the effect of flow on crystallization, it is useful to introduce the ratio Θ between the nucleation rate under quiescent conditions and that under flow. Use of eq 1 yields

$$\Theta \equiv \frac{\dot{N}_q}{\dot{N}_f} = \frac{1}{1 + \Delta G_f/\Delta G_q} \exp\left[\frac{K_n}{T(\Delta G_q)^n}\left(\frac{1}{(1 + \Delta G_f/\Delta G_q)^n} - 1\right)\right] \cong \frac{\vartheta_f}{\vartheta_q} \quad (20)$$

In eq 20, $\vartheta$ is the induction time, and subscripts "q" and "f" refer to quiescent and flow conditions, respectively. From now on, Θ is called dimensionless induction time. Obviously, under quiescent conditions Θ is unity, whereas Θ < 1 when flow is applied.

Equation 20 shows that Θ depends on both quiescent and flow parameters. In particular, under isothermal conditions, the quiescent parameters are the latent heat of fusion, $\Delta H_0$, the thermodynamic melting temperature, $T_m$, and the constant $K_n$. According to the models presented above, the flow parameters are a characteristic relaxation time ($T_d$ for the DE−IAA model, $\tau$ for the dumbbell models) and, under the reasonable approximation of constant polymer density, the molecular weight between entanglements, $M_e$.

Figure 3 reports the predictions of the DE−IAA model for the dimensionless induction time in both shear and uniaxial elongation. The curves in Figure 3 have been obtained by using the physical parameters of a linear polyethylene[21] and a crystallization temperature of 398 K, as indicated also in Table 1. For both types of flow, significant changes in the crystallization rate are predicted starting from Deborah numbers of order unity. For De > 1, a drop in Θ is observed, followed by a less steep region for higher De. As expected, the extensional flow is much more effective in enhancing the crystallization kinetics than the shear flow.

If eqs 11 and 12 are inserted into eq 20, the following explicit predictions for Θ in the low De limit are obtained for shear and elongational flow:

$$\Theta = \frac{1}{1 + C_1 De^2\pi^4/600} \exp\left\{C_2\left[\frac{1}{(1 + C_1 De^2\pi^4/600)^n} - 1\right]\right\} \quad (21)$$

$$\Theta = \frac{1}{1 + C_1 De^2\pi^4/200} \exp\left\{C_2\left[\frac{1}{(1 + C_1 De^2\pi^4/200)^n} - 1\right]\right\} \quad (22)$$

where

$$C_1 = \frac{3ckT}{\Delta G_q},\ C_2 = \frac{K_n}{T(\Delta G_q)^n} \quad (23)$$

Similarly, for high De

$$\Theta = \frac{1}{1 + C_1(\ln De - 2.41)} \exp\left\{C_2\left[\frac{1}{(1 + C_1(\ln De - 2.41))^n} - 1\right]\right\} \quad (24)$$

for shear flow and

$$\Theta = \frac{1}{1 + C_1(\pi^2 De/12 - 1)} \exp\left\{C_2\left[\frac{1}{(1 + C_1(\pi^2 De/12 - 1))^n} - 1\right]\right\} \quad (25)$$

for elongation.

The above equations can be very useful as they give analytical predictions of the induction time in the limit of slow and fast flows. They are reported in Figure 3 as dashed lines. It is apparent that, especially for the case of elongational flow, they reproduce the predictions of the exact calculations over a wide range of De. It should be reminded that the De values where the asymptotes are reached do depend on the material parameters of the specific polymer.

Figure 3 implicitly shows the effect of the polymer relaxation time on Θ. In fact, the relaxation time $T_d$ enters eq 20 only through the Deborah number (compare also eq 8). As a consequence, a change in $T_d$ is equivalent to a horizontal shift of the induction time curve when plotted in terms of the *dimensional* velocity gradient. The main factor determining the relaxation time of the polymer is in turn its molecular weight, $M$. It should be stressed here that the model predicts a dramatic dependency of the crystallization rate upon the molecular weight, as $T_d$ is a strong function of $M$ (typically,[34] $T_d \propto M^{3.4}$). It should be also pointed out that using a single relaxation time to describe the polymer behavior is obviously a crude approximation. The effects of polydispersity, for example, are not accounted for in the present formulation.

Figure 4 shows the effect of the molecular weight between entanglements, $M_e$, on the dimensionless induction time for the case of shear flow. Predictions for

**Table 1. Crystallization Parameters**

| polymer | ref | $\Delta H_o$ (J/m$^3$) | $T_m$ (K) | $T$ (K) | $n$ | $K_n$ [K (J/m$^3$)$^n$] | $\rho$ (kg/m$^3$) | $M_e$[35] | $T_d$ (s) | $\tau$ (s) |
|---|---|---|---|---|---|---|---|---|---|---|
| polyethylene | 21 | $2.8 \times 10^8$ | 418 | 398 | 2 | $8.7 \times 10^{17}$ | 980 | 828 | 0.46 | 0.38 |
| polypropylene | 21 | $1.4 \times 10^8$ | 481 | 394 | 1 | $2.0 \times 10^{11}$ | 970 | 4623 | 1.86 | 0.66 |
| polypropylene | 25 | $1.4 \times 10^8$ | 443 | 413 | 1 | $6.0 \times 10^{10}$ | 970 | 4623 | 10.1 | |
| | | | | 415 | | | | | 9.2 | |
| | | | | 418 | | | | | 8.3 | |
| polypropylene | 36 | $1.4 \times 10^8$ | 467 | 413 | 1 | $9.0 \times 10^{10}$ | 970 | 4623 | 40 | 10 |

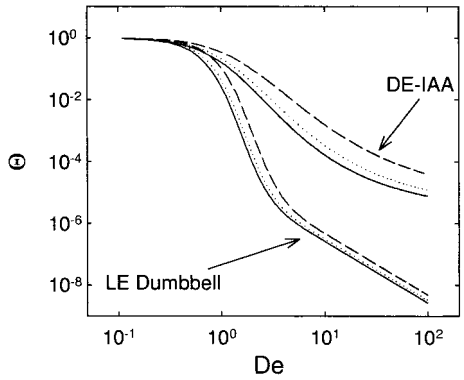


**Figure 4.** Dimensionless induction time as a function of De in shear flow for different values of $M_e$: (—) $M_e = 828$; (···) $M_e = 1000$; (- - -) $M_e = 1500$. The upper curves refer to the DE−IAA model. The lower curves refer to the LE dumbbell model.

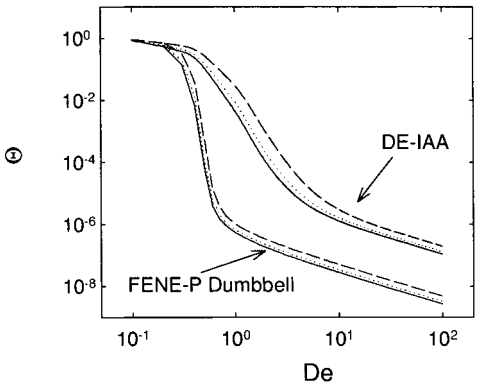


**Figure 5.** Dimensionless induction time as a function of De in uniaxial elongation for different values of $M_e$: (—) $M_e = 828$; (···) $M_e = 1000$; (- - -) $M_e = 1500$. The upper curves refer to the DE−IAA model. The lower curves refer to the FENE-P dumbbell model with $b = 100$.

both the DE−IAA and the LE dumbbell model are reported. The same comparison for uniaxial elongational flow is presented in Figure 5. In the latter, however, the results for the FENE-P model are reported, as the LE dumbbell unphysically diverges at De = 0.5. It can be seen that an increase in $M_e$ produces a less prominent FIC effect. This can be easily understood, as larger values of $M_e$ correspond to a smaller entanglement density and to a reduction in the number of oriented chain segments. It should be recalled that $M_e$ essentially depends on the polymer chemical structure.

From both Figures 4 and 5, the much stronger FIC effect predicted by the dumbbell models, as compared to the DE−IAA model, can be appreciated. In particular, the LE dumbbell in shear flow shows a four-decade drop in the induction time when the Deborah number changes by a mere factor of 3 (from De ≅ 1 to De ≅ 3). The situation is similar in elongation, where an even sharper drop of Θ is predicted by the FENE-P model for De ≅ 1, corresponding to the coil−stretch transition of the dumbbell configuration.

## 4. Comparison with Experiments

In this section the predictions of the DE−IAA model for FIC crystallization are compared with experimental results. It should be recalled that five parameters are present in the model, namely, the latent heat of fusion $\Delta H_0$, the melting temperature $T_m$, the constant $K_n$, the molecular weight between entanglements $M_e$, and the disengagement time $T_d$. In principle, all of them can be obtained by independent measurements, thus making the model fully predictive. In practice, as already mentioned in the previous section, $T_d$ is not sufficient to describe the whole relaxation behavior of a real polymer melt. Furthermore, in the experimental works on FIC, the rheological information necessary to obtain the relaxation time is almost always absent. For these reasons, in comparing the model with experiments, $T_d$ has been considered as the only adjustable parameter. Therefore, to perform a robust test of the model, comparisons were made only when the other four parameters were available from independent measurements. In this respect, no experimental data on elongational flow could be found, and the comparison is limited to the case of shear flow. A summary of the experimentally determined parameters for each set of data used in the comparison is reported in Table 1. As for $M_e$, values reported by Fetters et al.[35] have been used. In all cases, $T_d$ has been determined with a nonlinear fit of the data. To this end, a Levenberg−Marquardt algorithm has been used.

The first induction time data for FIC under steady shear flow date back to late 1970s. Lagasse and Maxwell[26] investigated the isothermal crystallization of two different polymers, a polyethylene (PE) and a polypropylene (PP). A parallel plate shear cell was used, and the shear flow was imposed after a well-defined quenching time. Induction times were measured by detecting the sharp rise of the melt viscosity under a steady shear flow. Experiments with PE were conducted at $T = 125$ °C, with a nominal melting temperature $T_m = 145$ °C. In this case, since the working temperature is relatively close to $T_m$, the authors determined a value of $n = 2$ (see eq 1). In the case of PP, the experiments were conducted at $T = 121$ °C, with a melting temperature $T_m = 208$ °C, and $n = 1$ was assumed.

Dimensionless induction times as a function of shear rate are plotted in Figures 6 and 7 for PE and PP, respectively, and are compared with the predictions of the DE−IAA model. In both cases the agreement between model and experiments is good. The best fit values of $T_d$ are reported in Table 1. In the same figures the predictions of the LE dumbbell model are also reported. As for the DE−IAA model, the only adjustable parameter is the relaxation time, $\tau$. The values of $\tau$ obtained from the regression procedure are also reported in Table 1. A much poorer agreement with the experimental data is found for the dumbbell model. In particular, as already outlined in the previous section, the dumbbell model largely overpredicts the enhancement in crystallization rate for De > 1.

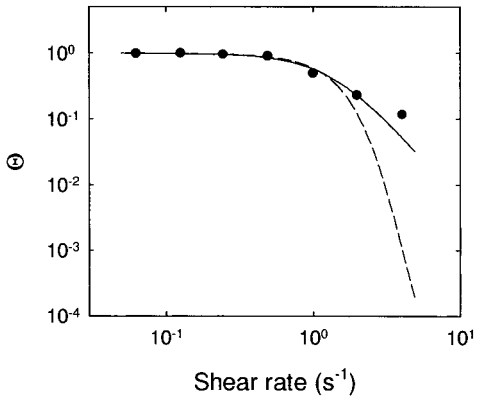


**Figure 6.** Dimensionless induction time as a function of shear rate for a polyethylene. Points are experimental data by Lagasse and Maxwell:[21] (—) DE−IAA model; (- - -) LE dumbbell model.

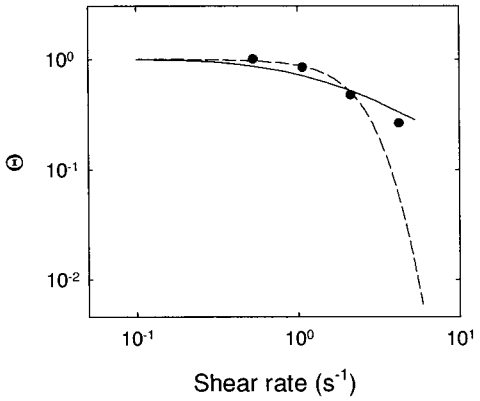


**Figure 7.** Dimensionless induction time as a function of shear rate for a polypropylene. Points are experimental data by Lagasse and Maxwell:[21] (—) DE−IAA model; (- - -) LE dumbbell model.

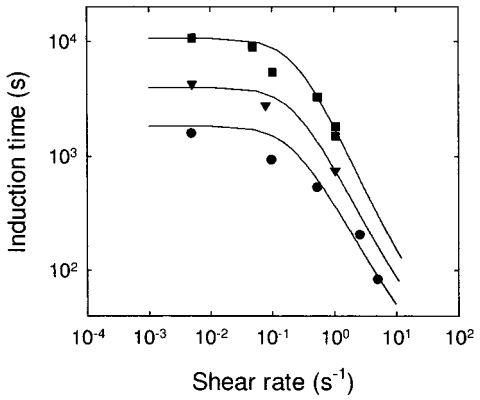


**Figure 8.** Induction time as a function of shear rate for a polypropylene at different temperatures. Points are experimental data by Nieh and Lee:[25] (■) 145 °C; (▼) 142 °C; (●) 140 °C. (—) DE−IAA model.

Figure 8 presents the comparison of the model with the FIC data of Nieh and Lee[25] for a polypropylene. The experimental induction time is obtained again as the time of sharp upturn of the viscosity curve at fixed shear rate. Data at different temperatures were collected. For their PP, Nieh and Lee indicate $T_m = 170$ °C and $n = 1$. Here the comparison is made only for temperatures where a clear plateau value for the induction time at low shear rates could be detected, namely, 140, 142, and 145 °C. In this case, for the sake of clarity, the comparison is made with the absolute induction time rather than its dimensionless value. The good agreement between model and experiments is confirmed. It should be added that, as reported in Table 1, the values of $T_d$ obtained from the best fit procedure show the correct dependency upon temperature, as higher temperatures correspond to shorter characteristic times. Even more remarkably, the calculated $T_d$'s show the same temperature dependence of the experimentally determined relaxation spectrum, as it was checked by using the shift factor determined by Nieh and Lee from linear viscoelastic measurements at different temperatures.[25] This fact represents a quantitative validation of the scaling behavior of the model with respect to the polymer relaxation time.

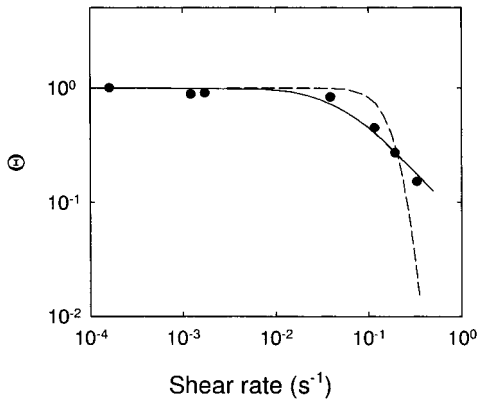


**Figure 9.** Dimensionless induction time as a function of shear rate for a polypropylene. Points are experimental data by Acierno et al.:[36] (—) DE−IAA model; (- - -) LE dumbbell model.

A further comparison is presented in Figure 9, where recent induction time data for a polypropylene[36] are plotted as a function of the shear rate. The experiments are conducted by means of a controlled stress rheometer equipped with cone and plate fixtures. As usual, the induction time is determined by the sudden change in the viscosity vs time curve. Quiescent DSC measurements were used to determine $K_n$ (with $n = 1$ in this case) and $T_m$ (see Table 1). FIC experiments were conducted at $T = 140$ °C. Once again, good agreement is found between the DE−IAA model and the experiments. At the same time, the unrealistic behavior of the LE dumbbell is confirmed. It should be also noted that the best fit value of the characteristic time, $T_d = 40$ s (see Table 1), compares well with the longest relaxation time of the polymer, $\tau_{max} \cong 100$ s, as determined experimentally from linear viscoelasticity measurements.[36]

## 5. Final Remarks

The Doi−Edwards model proves to be successful in describing the flow-induced enhancement in the crystallization rate of polymer melts under steady shear flow. We believe that this result is strictly related to the fact that crystallization can be accelerated by increasing *orientation*, rather than *stretching* of the polymer chains, as confirmed by experimental results at moderate deformation rates. In fact, for shear rates smaller than the reciprocal Rouse time, the polymer coil is expected to be in its unstretched configuration. The use of the independent alignment approximation allows to obtain closed-form expressions for the flow-induced free energy change of the system, thus producing explicit predictions for the crystallization induction time, which may be

useful in processing applications. A further merit of the model is that it requires the knowledge of few, in principle all non adjustable parameters.

This work has not the presumption to be at all exhaustive. One crucial point to be addressed is the importance of the polymer relaxation time, which has been still treated here has an adjustable parameter to fit the experimental data. Although it was shown that the calculated disengagement time compares well with the experimentally determined longest relaxation time, it is believed that an a priori estimate of such a parameter can be attempted by incorporating polydispersity of the polymer into the model.

It should be also stressed that a more severe test of the model requires the comparison with experimental data in flow conditions different from simple shear, such as uniaxial or planar elongation, which are technically important in processes like fiber spinning and filming.

**Acknowledgment.** The financial support of the Italian Ministry of University and Scientific Research, PRIN 1999-2001 "Flow-induced crystallization of polymers. Impact on processing and manufact properties", is gratefully acknowledged. The authors wish to thank S. Acierno and G. Alfonso for making available some of the experimental results before their publication, and G. Titomanlio for fruitful discussions.

## References and Notes

(1) *Flow Induced Crystallization*; Miller, R. L., Ed.; Gordon and Breach: London, 1979.
(2) Ziabicki, A.; Jarecki, L. In *High-Speed Fiber Spinning*; Ziabicki, A., Kawai, H., Eds.; Wiley: New York, 1985; p 225.
(3) Eder, G.; Janeschitz-Kriegl, H. *Mater. Sci. Technol.* **1997**, *18*, 296.
(4) Monasse, B. *J. Mater. Sci.* **1992**, *27*, 6047.
(5) Wassner, E.; Maier, R. D. In *Proc. XIII Int. Congr. Rheol.* **2000**, 1−183.
(6) Turnbull, D.; Fisher, J. C. *J. Chem. Phys.* **1949**, *17*, 71.
(7) Lauritzen, J. I.; Hoffman, J. D. *J. Revs. Natl. Bur. Stand.* **1960**, *64A*, 73.
(8) Eder, G.; Janeschitz-Kriegl, H. *Colloid Polym. Sci.* **1988**, *266*, 1087.
(9) Guo, X.; Isayev, A. I.; Guo, L. *Polym. Eng. Sci.* **1999**, *39*, 2096.
(10) Zuidema, H. Flow induced crystallization of polymers; Ph.D. Thesis, Technische Universiteit Eindhoven, Eindhoven, The Netherlands 2000.
(11) McHugh, A. J. *Polym. Eng. Sci.* **1982**, *22*, 15.
(12) Flory, P. J. *J. Chem. Phys.* **1947**, *15*, 397.
(13) Gaylord, R. J.; Lohse, D. J. *Polym. Eng. Sci.* **1976**, *16*, 163.
(14) Bushman, A. C.; McHugh, A. J. *J. Polym. Sci.: B: Polym. Phys.* **1996**, *34*, 2393.
(15) Doufas, A. K.; McHugh, A. J.; Miller, C. *J. Non-Newtonian Fluid Mech.* **2000**, *92*, 27.
(16) Doufas, A. K.; McHugh, A. J.; Miller, C.; Immaneni, A. *J. Non-Newtonian Fluid Mech.* **2000**, *92*, 81.
(17) Doi, M.; Edwards, S. F. *The Theory of Polymer Dynamics*; Clarendon Press: Oxford, England, 1986.
(18) Marrucci, G.; Grizzuti, N. *J. Rheol.* **1983**, *27*, 433.
(19) Ziabicki, A. *Colloid Polym. Sci.* **1996**, *274*, 705.
(20) Pearson, D.; Herbolzheimer, E.; Grizzuti, N.; Marrucci, G. *J. Polym. Sci.: B: Polym. Phys.* **1991**, *29*, 1589.
(21) Lagasse, R. R.; Maxwell, B. *Polym. Eng. Sci.* **1976**, *16*, 189.
(22) Pucci, M. S.; Carr, S. H. *Polym. Sci. Technol.* **1983**, *22*, 139.
(23) Vleeshouwers, S.; Meijer, H. E. H. *Rheol. Acta* **1996**, *35*, 391.
(24) Bushman, A. C.; McHugh, A. J. *J. Appl. Polym. Sci.* **1997**, *64*, 2165.
(25) Nieh, J.; Lee, L. J. *Polym. Eng. Sci.* **1998**, *38*, 1121−1132 and 1133−1141.
(26) Floudas, G.; Hilliou, L.; Lellinger, D.; Alig, I. *Macromolecules* **2000**, *33*, 6466.
(27) Mead, D. W.; Larson, R. G.; Doi, M. *Macromolecules* **1998**, *31*, 7895.
(28) Marrucci, G. *J. Non-Newtonian Fluid Mech.* **1996**, *62*, 279.
(29) Ottinger, H. C.; Beris, A. N. *J. Chem. Phys.* **1999**, *110*, 6593.
(30) Bird, R. B.; Hassager, O.; Armstrong, R. C.; Curtiss, C. F. *Dynamics of polymeric liquids*; Wiley: New York, 1977, Vol. II.
(31) Lodge, A. S. *Elastic liquids. An introductory vector treatment of finite-strain polymer rheology*; Academic Press: London, 1964.
(32) Sarti, G. C.; Marrucci, G. *Chem. Eng. Sci.* **1973**, *28*, 1053.
(33) Peterlin, A. *J. Chem. Phys.* **1960**, *36*, 1799.
(34) Ferry, J. D. *Viscoelastic properties of polymers*; Wiley: New York, 1980.
(35) Fetters, L. J.; Lohse, D. J.; Richter, D.; Witten, T. A.; Zirkel, A. *Macromolecules* **1994**, *17*, 4639.
(36) Acierno, S.; Alfonso, G.; Grizzuti, N. Manuscript in preparation.

MA010275E